Applied Catalysis B: Environmental 90 (2009) 652–661

Contents lists available at ScienceDirect

Applied Catalysis B: Environmental

journal homepage: www.elsevier.com/locate/apcatb

Catalytic treating of gas pollutants over cobalt catalyst supported on porous carbons derived from rice husk and carbon nanotube

Chi-Yuan Lu [a], Ming-Yen Wey [b,*], Kui-Hao Chuang [b]

[a] Department of Public Health, Chung Shan Medical University, Taichung 402, Taiwan, ROC
[b] Department of Environmental Engineering, National Chung Hsing University, No. 250, Kuo Kuang Road, Taichung 402, Taiwan, ROC

ARTICLE INFO

Article history:
Received 18 September 2008
Received in revised form 5 April 2009
Accepted 30 April 2009
Available online 6 May 2009

Keywords:
Porous carbon
Carbon nanotube
Carbonization
Catalyst

ABSTRACT

Porous carbons were prepared from rice husks, commercial coconut-shell-derived carbon, and carbon nanotube (CNT) by activation with CO_2, KOH, and $ZnCl_2$. Cobalt catalysts were supported on the six different porous carbons by excess-solution impregnation, and were used to carry out reactions with different constituents such as NO + CO, toluene, NO + toluene, and NO + CO + toluene in the presence of 6% O_2 at 250 °C to evaluate the activity of porous catalysts. The properties of the catalysts were analyzed by X-ray powder diffractometer (XRD), a field-emission scanning electron microscope (FESEM), transmission electron microscope (TEM), and an X-ray energy dispersive spectrometer (EDS). The cobalt catalysts supported on rice-husk-based carbon activated by CO_2 and those on commercial-activated-carbon re-treated by KOH showed 100% conversion on toluene oxidation. CNT-cobalt catalyst showed 63% NO conversion with CO and 46% with toluene at 250 °C. Among the six porous supported catalysts, the cobalt catalysts prepared with CNT and rice-husk-derived carbon by using CO_2 showed the best catalytic activity and thermal stability when compared to the others.

1. Introduction

Recently, activated carbon (AC) has also been widely used for catalytic supports because it has many advantages as a support due to its superior antacid and antalkali properties, high surface area, high pore volume and high mesoporosity [1–3]. Generally, ACs are produced from various carbonaceous materials such as animal bone, coal, coconut shell, pistachio shell, walnut shell, saw dust, wood, polymer scrap, industrial or municipal wastes, and refuse-derived fuel [4–9]. The method of preparation of AC involves two steps: the carbonization of the raw carbonaceous material in an inert atmosphere and the activation of the carbonized product. Various types of ACs with different pore size distributions can be obtained by using different raw materials and activation methods.

The activation methods can be classified into physical and chemical activation [10,11]. The former involves heating the carbonaceous materials at a high temperature with a reactant such as CO_2 and H_2O [12–15]. The latter involves heating the carbonaceous material at relatively low temperatures with the addition of activating agents such as H_3PO_4, $ZnCl_2$, K_2CO_3, and KOH [16–22]. AC mainly consists of micropores with mesopores and macropores present in only small ratios. For catalytic applications, the carbon support should possess not only a high surface area but also high mesoporosity. Several studies have reported that mesopores significantly enhance the catalytic activity of materials by allowing macromolecules to penetrate them and get easily adsorbed on the surface of the catalyst [23–25]. Therefore, it is essential to modify the pore texture of ACs and increase their mesoporosity for their use catalyst supports. There are several reports on the development of mesoporous carbons and the factors that influence their formation, including the carbonaceous materials used, pretreatment, nature of activating agent, ratio of activating agents/carbonaceous material, carbonization temperature, carbonization time, acid treatment etc. [23–27]. $ZnCl_2$ and KOH are some of the chemical activating agents commonly used in the preparation of activated carbon. Yang et al. [28] prepared 57% mesoporous AC (2970 $m^2\ g^{-1}$) from mesophase pitch by heating it with KOH (pitch/KOH = 1/7) at 780 °C for 4 h in N_2 atmosphere. Hayashi et al. [29] prepared 30% mesoporous AC (1778 $m^2\ g^{-1}$) from chickpea husks by chemical activation at 800 °C for 1 h in N_2 with K_2CO_3 (husk/K_2CO_3 = 2). In addition to activation of carbon products, these chemical and physical processes help to enlarge the ratio of their mesoporous content [30,31]. The $ZnCl_2$ chemical activation method (shell/$ZnCl_2$ = 3) is proposed to produce 71% mesoporous content (ratio of mesopore volume to total pore volume) AC (2400 $m^2\ g^{-1}$) from coconut shells at 800 °C for 2 h in CO_2 [11]. Due to the advantages of higher mesoporous content

* Corresponding author. Tel.: +886 4 22852455; fax: +886 4 22862587.
E-mail address: mywey@dragon.nchu.edu.tw (M.-Y. Wey).

0926-3373/$ – see front matter © 2009 Elsevier B.V. All rights reserved.
doi:10.1016/j.apcatb.2009.04.030

carbons, the numbers of reported studies in this field have been increasing.

Although there are several studies that focus on enhancing the mesoporous content of AC, most applications of more mesoporous content carbons concern the removal of pollutants from gas or wastewater via adsorption [32–34]. Very few works were reported with regard to the utilization of transition-metal catalysts supported on more mesoporous content carbons for the catalytic removal of gas pollutants in flue gas at low temperatures. In addition, not many researchers studied the simultaneous removal of VOC, CO, and NO in the incinerator flue gas. Therefore, the purpose of this work was to study mesoporous content carbons as supports for cobalt catalysts to be used in VOC oxidation. In this study, the porous carbons were prepared from three types of carbonaceous materials; rice husk, commercial coconut-shell-derived carbon, and carbon nanotube (CNT); rice husk was selected because it is a major waste product obtained from the rice milling industry in Taiwan and accounts for approximately 20% of the whole rice grain. Wang et al. [35] and Huang et al. [36] reported that CNT-supported catalysts (Pd/CNTs and V_2O_5/CNT) showed the high catalytic activity for NO reduction. Further, we evaluated the catalytic activities of the high mesoporous content catalysts were also evaluated in different atmospheres: NO + VOC, CO + NO, and CO + NO + VOC.

2. Experimental

2.1. Preparation of porous carbon support

In the experiment, we chose rice husks, commercial AC, and CNT as carbon supports. Six types of carbon supports were prepared with different conditions as follows. First, rice husks were washed with deionized water and dried at 110 °C for 24 h and then grounded. The commercial AC was prepared from a commercial coconut-shell-derived carbon (purchased from China Activated Carbon Industries Ltd. in Taiwan) through physical steam activation at approximately 800 °C. A particle size of 0.335 mm was obtained by sieving. Subsequently, the precursors were impregnated with an activation solution of $ZnCl_2$ and KOH. The weight ratios of chemical precursor are listed in Table 1. $RHZnCl_2$ and RHKOH denote rice-husk-based carbon activated by $ZnCl_2$ and KOH. $ACZnCl_2$ and ACKOH denote commercial-activated-carbon re-treated by $ZnCl_2$ and KOH. The mixtures were dried in an oven overnight at 110 °C and then heated in a tube furnace under a nitrogen flow of 500 ml min^{-1}. For $RHZnCl_2$ and $ACZnCl_2$, the temperature was raised from the ambient temperature to 550 °C at 10 °C min^{-1}, and the activation was continued for 1 h. For RHKOH and ACKOH, the temperature was ramped from the ambient temperature to 800 °C at 10 °C min^{-1}, and the activation was continued for 1 h. The carbon supports were then cooled to room temperature and soaked in HCl for 24 h to remove the remaining chemicals until the washed solution was free of zinc or potassium cations. Subsequently, they were washed and dried with deionized water at 110 °C for 24 h.

$RHCO_2$ denotes rice-husk-based carbon activated by CO_2. The temperature was ramped from room temperature to 300 °C and then to 500 °C at 10 °C min^{-1} with a nitrogen flow of 500 ml min^{-1} and held for 1 h at each temperature. The temperature was then raised to 850 °C at 10 °C min^{-1}. When the temperature reached 850 °C, the gas flow was switched to 500 ml min^{-1} of CO_2, and the activation was continued for 2 h. The $RHCO_2$ was washed with deionized water to remove the remaining impurities and dried at 110 °C for 24 h.

Finally, the CNTs were grown from the Ni nanoparticles by chemical vapor deposition (CVD) method at 700 °C with C_2H_2 (H_2:C_2H_2 = 6:1) for 1 h. Then the CNT was soaked in the acid solution (H_2SO_4:HNO_3 = 1:3) for 24 h to remove Ni, washed and dried at 110 °C for 24 h.

2.2. Catalyst preparation

Porous catalysts were all prepared by excess-solution impregnation using $Co(NO_3)_2{\cdot}6H_2O$ of appropriate concentration to obtain around 5 wt% metal content with six types of carbon supports previously prepared. During the impregnation, the solutions were heated at 70 °C with continuous stirring until all the liquid was evaporated. Then the catalysts were dried at 110 °C for 2 h and calcined at 500 °C for 4 h in the presence of hydrogen to get the catalysts.

2.3. Activity test

Fig. 1 depicts the reactor system used in this experiment. Catalytic activity measurements for the activity test were conducted at atmospheric pressure in a micro-catalytic reactor under a steady-state condition. In this study, the activity tests were carried out in the different reaction atmospheres (NO/CO/toluene). Toluene/nitrogen mixture was chosen to represent one of the VOC pollutants. The toluene vapor was carried by nitrogen from a saturator filled with liquid toluene. The concentration of toluene was 150 ppm, which was adjusted by the temperature of saturator and mixed air flow rate. The reactor was a 9 mm ID quartz tube, and the catalysts were placed on quartz filter board. Sample weight of ca 992 mg and flow rates of 500 ml min^{-1} of the feed gas governed by Brooks mass flow controller were used for the activity test. A thermocouple was placed in the center of catalyst bed to record reaction temperature and also used to control the furnace. Both reactants and products were both monitored by gas chromatograph/flame ionization detector (Agilent, GC-6890N) and an online flue gas analyzer (Horiba, PG-250). Thus, the conversion was calculated based on toluene consumption from the inlet and outlet concentrations of toluene.

2.4. Characterization of catalysts

Several experimental analyzers were used to characterize the samples. An X-ray diffractometer (XRD) (SIEMENS D5000) equipped with a Cu tube served as the X-ray source was employed to estimate the active site phase, and the working voltage and current was 30 V and 20 A, respectively. The powdered samples were pressed onto suitable holders and were scanned within the 2

Table 1
Preparation conditions of various carbon supports.

Sample	Carbon source (W1)	Agent (W2)	Ratio (W2/W1)	Carbonization temperature (°C)
$RHCO_2$	Rice husk	CO_2	–	850
$RHZnCl_2$	Rice husk	$ZnCl_2$	2	550
RHKOH	Rice husk	KOH	2	800
$ACZnCl_2$	Commercial AC	$ZnCl_2$	0.5	550
ACKOH	Commercial AC	KOH	0.5	800

theta (2θ) range 20–80°, in steps of 0.04°. The scanning speed was $4^\circ\ min^{-1}$.

Particle size, powder morphologies and elemental structure of the loadings were investigated using field-emission scanning electron microscopy (FESEM) and transmission electron microscope (TEM). FESEM (JSM-6700F, JEOL) operated at 5 kV accelerating voltage and equipped with X-ray energy dispersive spectrometer (EDS) facility.

TEM observations were made with a JEOL JEM-1400 microscope operated at 120 kV to observe the dispersion of cobalt particles on the carbon supports. The samples were crushed in an agathe mortar and suspended in ethanol. After ultrasonic dispersion, a droplet was deposited on a copper grid supporting a perforated carbon film.

The surface area of the catalysts was measured at 77 K by gravimetric methods with an ASAP 2010 vacuum microbalance. It provides area comparisons for catalysts prepared at different reduction times. N_2 adsorption–desorption of surface was used to determine the textural properties. The Brunauer–Emmett–Teller (BET) surface area was calculated from the adsorption isotherm. The average pore diameter was obtained from the pore size distribution.

For determining the composition of elements on the porous carbon support, the elemental analysis of catalysts was carried out by a CHNO-RAPID elemental analyzer (EA). The weight percentages of C, H, N, and O in the catalyst were determined.

3. Results and discussion

3.1. Characteristics of the porous carbon supports

The parameters describing the porous texture of the six porous carbon supports, which were calculated from their corresponding isotherms with commercial AC as reference, are given in Table 2. Fig. 2 shows pore volume ratio obtained by different preparation methods; it is found that the distribution of the mesopore volume obtained from rice husk was 40% in the case of $RHCO_2$ and RHKOH and 20% in the case of $RHZnCl_2$. The average pore diameter is in the following order: $RHCO_2$ (41.3 Å) > RHKOH (36.9 Å) > $RHZnCl_2$ (27.1 Å). On the contrary, the specific surface area was in the following order: $RHZnCl_2$ > RHKOH > $RHCO_2$. The maximum specific surface area obtained was 1555 $m^2\ g^{-1}$. These results show that $ZnCl_2$ had a higher ability to prepare carbon supports with high specific surface area from rice husks than other activating agents. The activating agents KOH and CO_2 had better efficiency in enhancing the mesoporous content when compared with $ZnCl_2$ for rice-husk pretreatment. In past studies, ACs with specific surface area (S_{BET}) values in the range of 150–2000 $m^2\ g^{-1}$ have been prepared from rice husks, which is consistent with the S_{BET} values obtained in this study [33,37,38].

Previous studies [11,30,31] indicate that combining chemical activation with physical activation can improve the mesoporous volume of carbonaceous materials. Because commercial AC is prepared from a coconut-shell-derived carbon only via physical steam activation, we carried out its secondary treatment with $ZnCl_2$ and KOH. It was found that the modification of AC by $ZnCl_2$ and KOH resulted in an increase in both the pore size and S_{BET} value. The secondary treatment of AC by chemical activation showed only a slight improvement in the mesoporous content of the carbon support. ACKOH showed a better pore size (32.9 Å) with an S_{BET} value of 1008 $m^2\ g^{-1}$ than $ACZnCl_2$.

In addition, we also prepared CNT to serve as porous carbon support. On analysis of BET surface area, the CNT showed better mesoporous distribution than others materials. The ratio of mesopore volume obtained is 70% as shown in Fig. 2, and in contrast, the CNT had the smallest specific surface area of 65.1 $m^2\ g^{-1}$. A comparison of the average pore diameter of all carbon supports revealed that CNT had the largest diameter of 76.4 Å, while the pore sizes of the other materials were in the following order: $RHCO_2$ > RHKOH > ACKOH > $RHZnCl_2$ > $ACZnCl_2$. Thus, the mesoporosity distributions of all the six porous carbons were higher than that of commercial AC (Table 2).

The elemental composition of the porous carbons prepared by different activation methods is given in Table 3. Carbon, hydrogen,

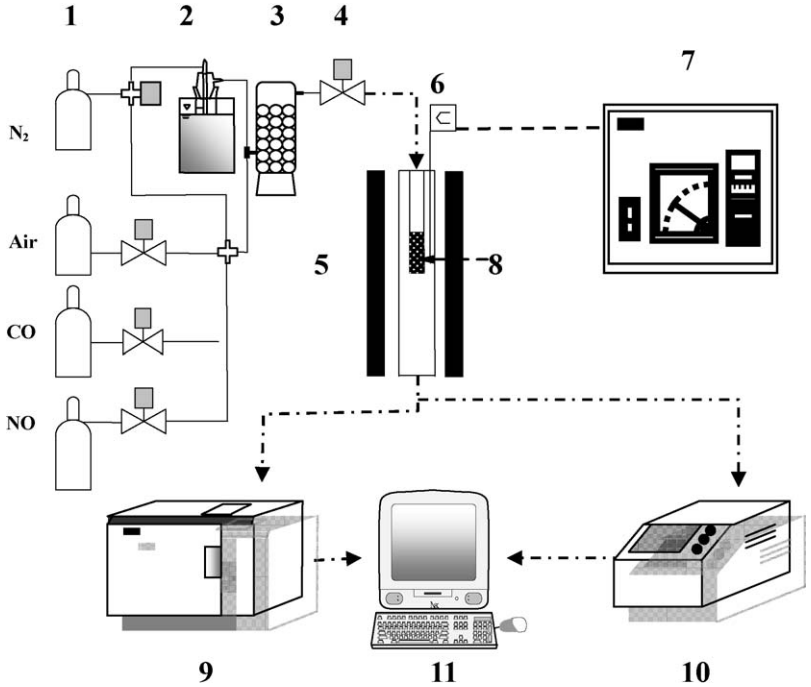

Fig. 1. Schematic diagram of reactor system: (1) gas cylinder; (2) cooling tank, saturator, and toluene; (3) gas mixed room; (4) mass flow controller; (5) tube reactor; (6) thermocouple; (7) temperature feedback control; (8) catalyst; (9) GC; (10) non-dispersive infrared analyzer; (11) data logger.

Table 2
BET surface area and structural characteristics of the various carbon supports.

	Sample						
	$RHCO_2$	$RHZnCl_2$	RHKOH	$ACZnCl_2$	ACKOH	CNT	AC
Specific surface area ($m^2\ g^{-1}$)	301.5	1555.0	936.0	1030.0	1008.0	65.1	1057.4
Pore volume ($cm^3\ g^{-1}$)	0.17	1.06	0.51	0.50	0.48	0.44	0.39
BJH average radius (Å)	41.3	27.1	36.9	21.8	32.9	76.4	19.4

Table 3
Chemical composition of carbon supports and used cobalt catalysts[a] expressed in %.

Element composition (%)		RH	$RHCO_2$	$RHZnCl_2$	RHKOH	$ACZnCl_2$	ACKOH	CNT
N%	Support	0.19	0.68	0.99	2.23	0.58	0.29	0.19
	Catalyst	–	0.29	0.27	0.00	0.11	0.23	0.11
C%	Support	40.56	49.57	47.25	50.56	91.27	91.40	95.60
	Catalyst	–	39.44	55.47	15.94	60.22	64.16	89.32
H%	Support	5.17	1.09	0.95	1.65	0.72	0.92	0.52
	Catalyst	–	2.06	2.98	2.47	2.74	2.70	2.11
O%	Support	38.45	28.29	32.24	39.60	7.23	7.27	3.69
	Catalyst	–	15.09	6.74	15.09	23.03	20.65	1.67
Others%	Support	15.63	20.37	18.57	5.96	0.20	0.12	0.00
	Catalyst	–	43.13	34.56	66.51	13.91	12.27	6.81

[a] Six types of cobalt catalysts reacted in NO + CO reaction.

oxygen, and nitrogen were found in all six porous carbons. Commercial AC-based carbons and CNT had a higher percentage of carbon (91%) than rice-husk-based porous carbons (50%). Moreover, from the raw composition of rice husk, it is clear that the composition did not change significantly after activation and carbonization. This result agrees with earlier studies [39], in which 50% of the carbon content is attributed to 20% ash, 38% cellulose, 22% lignin, 18% pentose, and 2% other organic components, which are present in rice husk.

3.2. Catalyst characterization

The FESEM images showing the surface morphologies of the porous carbons are shown in Fig. 3. The morphologies of the carbon materials prepared from rice husks are typical (Fig. 3(a)–(c)). It can be observed that the granules are extremely porous, and it is observed that the activating agents KOH and CO_2 showed better efficiency when compared with $ZnCl_2$ in developing the mesoporosity from rice husks. The same result is observed in the case of commercial AC after secondary treatment, as shown in Fig. 3(d) and (e). These results can be confirmed by BET analysis, as shown in Table 2 and Fig. 2. Thus, it is deduced that the mesoporosity can be effectively developed from commercial AC or rice husk using KOH or CO_2. For CNTs preparation, Serp et al. [40] reported that the difference between nanotubes and nanofibers consists in the lack of an hollow cavity for the latter. One can see that prepared CNTs by CVD method were a classic type of CNTs with hollow tubes.

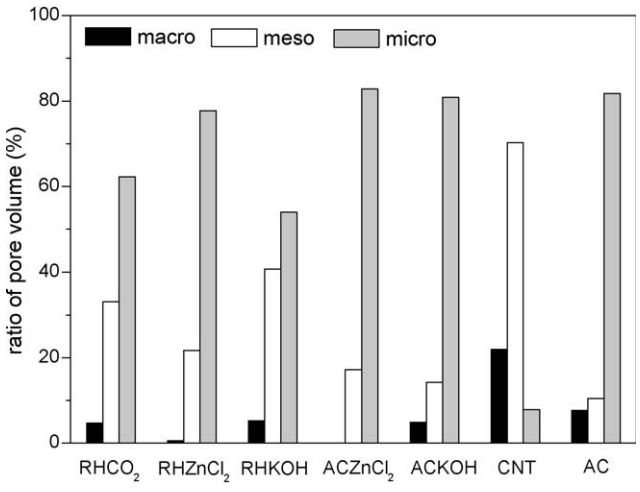

Fig. 2. The distribution of pore volume on various carbon supports.

Fig. 4 presents the TEM images of cobalt catalysts supported on different porous carbons, which were prepared by the impregnation method. It is observed that the cobalt particles were well dispersed on the rice-husk-based carbons, and the size of the cobalt particles were found to be in the nanoscale range (3–7.5 nm), as shown in Fig. 4(a)–(c). Fig. 4(d) and (e) presents the FESEM images of the Co catalysts supported on commercial AC-based carbons after the secondary treatment of the ACs; the cobalt particles supported on ACKOH and $ACZnCl_2$ were well dispersed. For CNT-cobalt catalyst, it can be observed that Co/CNT shows a fine dispersion of Co particles (8 nm), and some Co particles are into the hollow tubes, as shown in Fig. 4(f). It was concluded that cobalt particles supported six types of carbon supports were well dispersed and the sizes were within 100 nm. The average sizes of the Co particles follow the order: $RHCO_2$ (3 nm) < RHKOH (4 nm) < $RHZnCl_2$ (7.5 nm) < CNT (8 nm) < $ACZnCl_2$ (20 nm) < ACKOH (40 nm).

As compared to previously reported catalysts prepared by impregnation [41], ACKOH and $ACZnCl_2$ supports showed some advantageous properties. Besides the active sites had a good distribution; the size of metal particles obtained was 20–40 nm. From a previous study [42], it is considered that the hydrophilic functional groups O–H, C=O, and C–O were grafted on the carbon surface as a result of the secondary treatment that modifies the adsorption characteristics of the carbon.

In order to confirm the presence of small particles on the porous carbon supports, a small region (1 μm) on the samples was analyzed EDS. Fig. 5 shows the EDS pattern of the $ACZnCl_2$-cobalt catalyst, which shows the presence of carbon, oxygen, and cobalt; the peak for the metal active phase was weaker than that of carbon. Moreover, to confirm the crystalline structure of cobalt on the

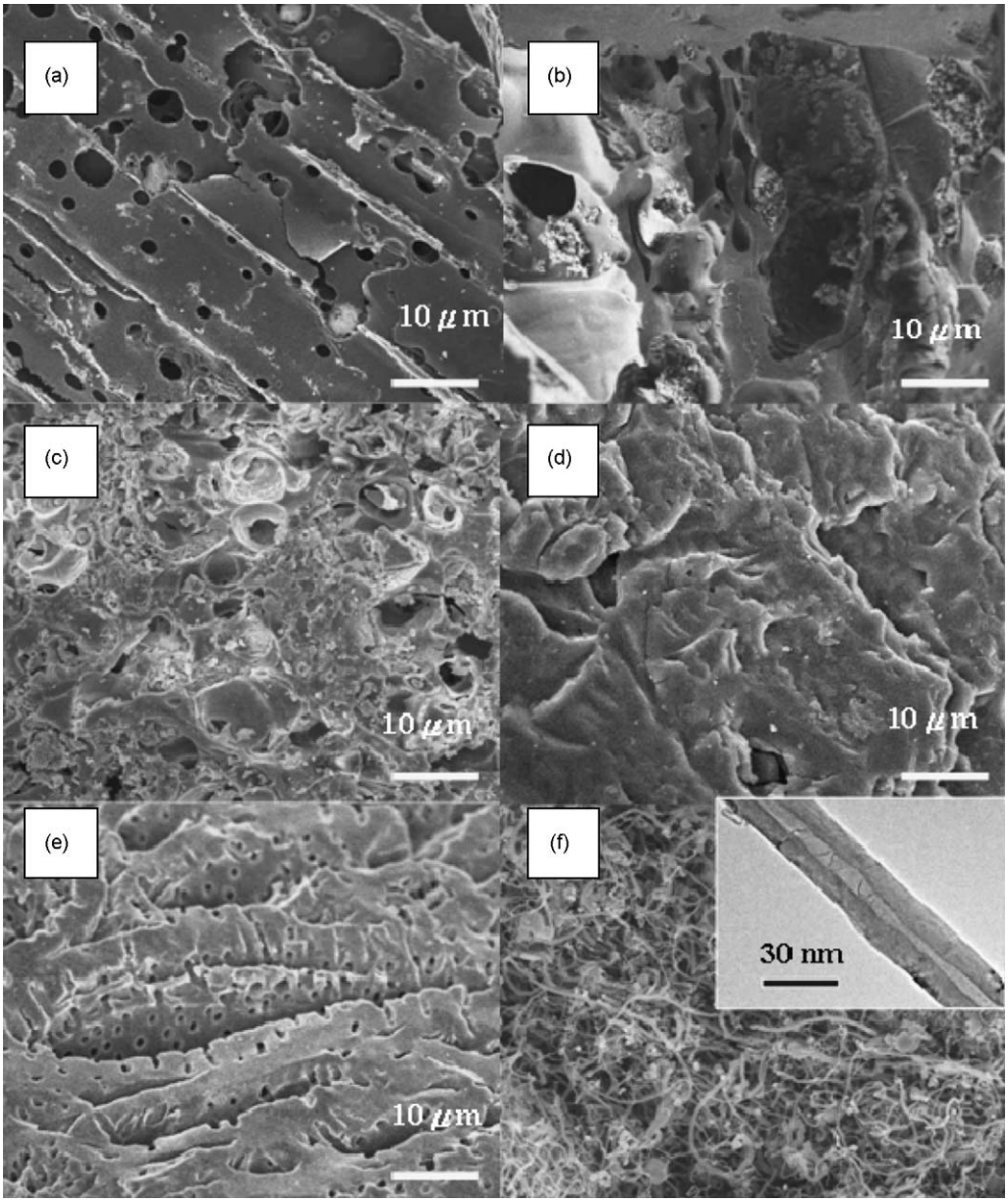

Fig. 3. SEM images of different carbon supports: (a) $RHCO_2$, (b) $RHZnCl_2$, (c) RHKOH, (d) $ACZnCl_2$, (e) ACKOH, and (f) CNT.

supports, XRD analysis was also performed. No apparent difference was observed in the patterns of the six catalysts on different carbon supports prepared by the impregnation process. Unclear peaks were detected for the cobalt species in Co/carbon supports showing that the structure of cobalt in the catalysts was amorphous. This also implied that the active phase was well dispersed on all catalysts. Several studies [43,44] have revealed that the intensity of the peaks decreases because of lower metal loading and good dispersion. The TEM images (Fig. 4) we obtained reveal that the nanoparticles are well dispersed on the support. Thus, XRD, TEM, FESEM, and EDS results have confirmed that the catalysts prepared with high mesoporous content supports show enhanced dispersion characteristics.

3.3. Catalytic activity test

3.3.1. VOC oxidation

In this study, the six porous carbons were prepared as supports for cobalt catalysts using conventional impregnation method. The toluene conversion of the six catalysts at 250 °C is shown in Fig. 6. On comparing the six catalysts, it was observed that porous catalysts showed better activity on VOC oxidation at 250 °C when compared to the obtained in previous works [45]. It was concluded that the catalytic activity increases when an active site is impregnated on a high mesoporous content carbon support, which results in high distribution of cobalt and facilitates the penetration of macromolecules and ions in the surface of the carbon support [23–25].

Among the six cobalt catalysts, those supported on $RHCO_2$ and ACKOH showed high efficiency of toluene conversion; the activity of the cobalt catalysts was observed to follow the order: $RHCO_2$, ACKOH > RHKOH > CNT > $RHZnCl_2$ > $ACZnCl_2$. Moreover, the activity test results can be compared with the BET analysis results. In the case of the catalysts supported on rice-husks-based carbons, it was observed that $RHZnCl_2$ showed higher specific surface area and larger pore volume than the others (Table 2). In theory, the $RHZnCl_2$ catalyst exhibited highest toluene-adsorption capacity due to its high S_{BET} and large pore volume. However, $RHCO_2$ and RHKOH catalysts showed better catalytic activity than $RHZnCl_2$.

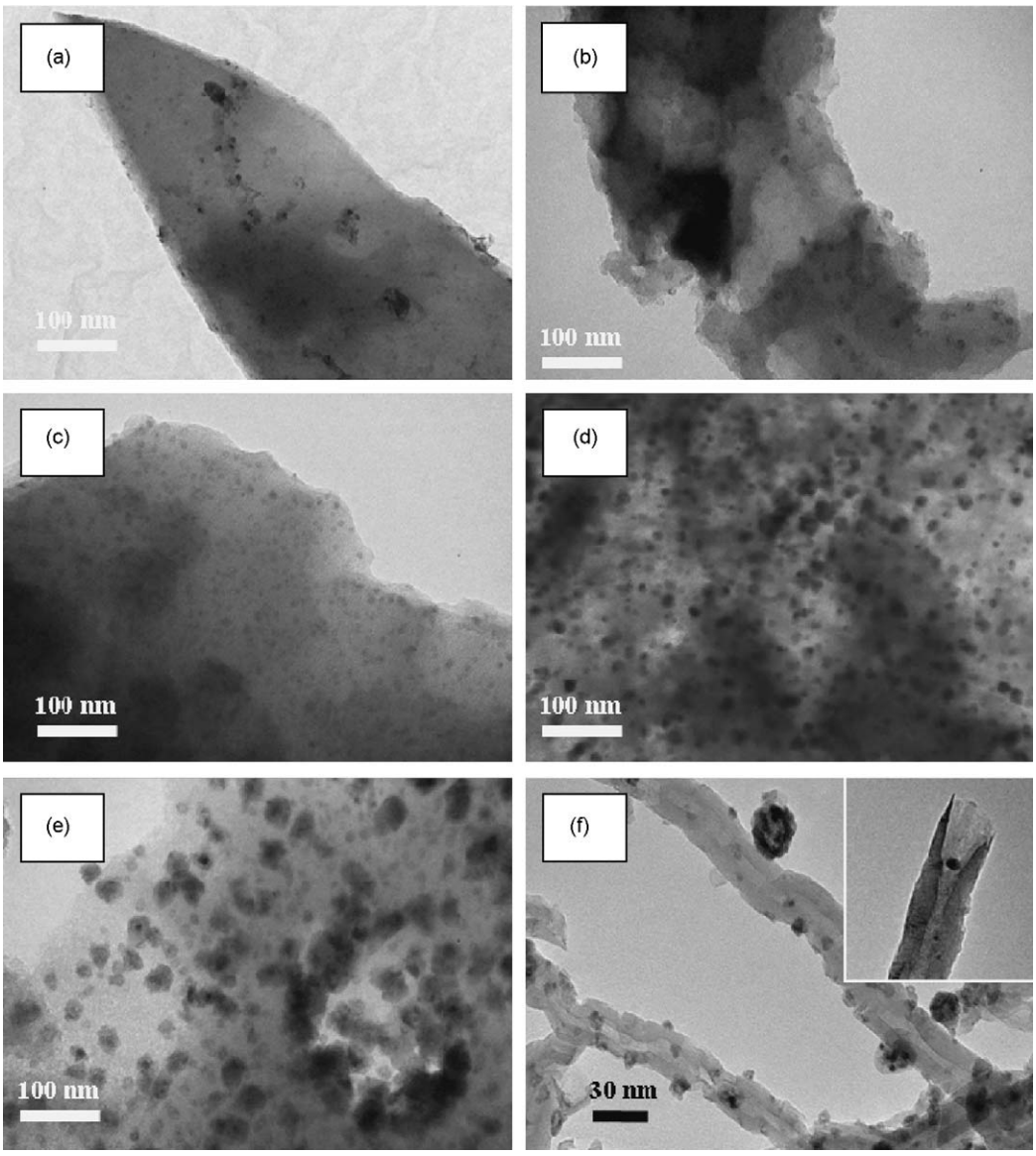

Fig. 4. TEM images of cobalt catalysts with different carbon supports: (a) $RHCO_2$, (b) $RHZnCl_2$, (c) RHKOH, (d) $ACZnCl_2$, (e) ACKOH, and (f) CNT.

The catalyst weights were measured before and after catalytic reaction in different reaction atmospheres and are listed in Table 4. Some types of catalyst weights were lost after reaction. From previous studies, it was found that this was due to the fact that Co exhibited a high catalytic activity in the presence of oxygen [46]. The oxidation of toluene oxidation over cobalt catalyst is exothermic. Since carbon supports cannot withstand the heat generated from the exothermic reaction of toluene-O_2-cobalt at 250 °C, the carbon supports were burnt off. Fig. 7(a) and (b) shows the variation of CO and CO_2 in the stream produced while toluene was oxidized catalytically. In Fig. 8(a), it is observed that during the initial 50 min of the reaction, $RHZnCl_2$ released a large amounts of CO_2 as compared to $RHCO_2$ and RHKOH; this also explained why the weight of the $RHZnCl_2$ catalyst decreased from 0.992 g to 0.713 g after the reaction. After the catalytic support was burnt off (after 50 min), the efficiency of toluene oxidation returned to normal. The maximum CO_2 concentration of 700 ppm was released by the $RHCO_2$-cobalt catalyst. On comparing the TEM images of the cobalt catalysts (Fig. 4(a)–(c)), it is observed that the size of the active phase on $RHZnCl_2$ was greater (7.5 nm) than that of the others, even though the active phase in all cases were well dispersed. Besides, it is well known that the activated carbon may adsorb large amounts of VOCs due to its high specific area and large pore volume; therefore, it can be suggested that the $RHZnCl_2$ catalyst adsorbed large amounts of toluene as compared to others. Form the above two points, it can be concluded that $RHZnCl_2$ cannot withstand the large amount of heat generated as the exothermic reaction of toluene-O_2-Co proceeds rapidly. Therefore, the low conversion of $RHZnCl_2$ in VOC oxidation can be attributed to its large active-phase size, high specific surface area, and large pore volume.

Among the supports prepared from commercial ACs after secondary treatment, the ACKOH catalyst showed better activity than $ACZnCl_2$. The low toluene conversion of $ACZnCl_2$ was a result of the burn-off reaction of the catalyst; further 40% of the weight was lost after toluene oxidation. As discussed above, this loss in weight was attributed to the particle size of cobalt, dispersion of the active phase, and the pore volume of the carbon support. From Fig. 4(d) and (e) and Table 2, it can be deduced that the $ACZnCl_2$-cobalt catalyst may be burnt off cause of the higher density of the active phases than ACKOH-cobalt catalyst. $ACZnCl_2$ cannot withstand the heat generated from the exothermic reaction of toluene oxidation at 250 °C. Besides, the weight loss of commercial AC-based catalysts was more

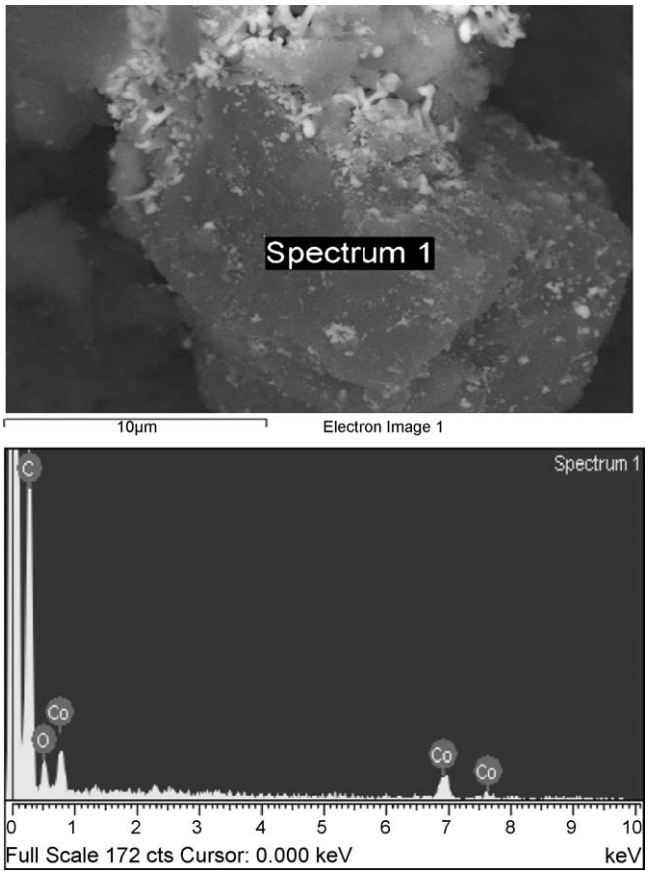

Fig. 5. (a) FESEM image of the $ACZnCl_2$-cobalt catalyst and (b) EDS analysis of the crystallite.

than that of rice-husk-based catalysts. This was because the carbon content in commercial AC-based support was 91% (Table 3), while that of rice-husk-based one was 50%; as a result the former undergoes an increased weight loss during the burn-off reaction. The CNT catalyst showed a conversion efficiency of 72% in VOC oxidation with good thermal stability, even though its carbon content is as high as that of commercial AC-based catalysts.

Further, the selectivity of toluene oxidation was evaluated from the variation of CO and CO_2 concentrations in the stream during oxidation, as shown in Fig. 7(a) and (b). The results show that the

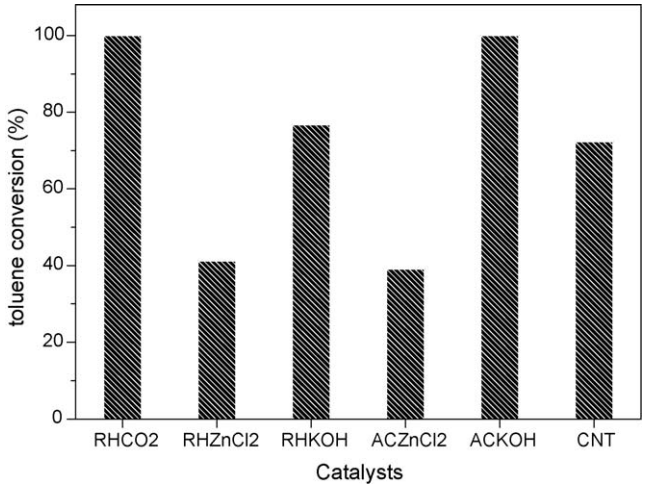

Fig. 6. The toluene conversion with different supports on cobalt catalysts tested at 250 °C (feed composition: 150 ppm toluene, SV = 40,000 h^{-1}, and 6% O_2 in N_2).

Table 4
Weight variation of fresh and used cobalt catalysts.

Catalyst	Reaction atmosphere							
	Toluene		NO + toluene		NO + CO		NO + CO + toluene	
	Fresh	Used	Fresh	Used	Fresh	Used	Fresh	Used
$RHCO_2$	0.992	0.972	0.992	0.975	0.992	0.996	0.992	1.005
$RHZnCl_2$		0.713		0.519		0.959		1.002
RHKOH		0.86		0.786		0.736		0.825
$ACZnCl_2$		1.003		0.357		0.361		0.769
ACKOH		0.596		0.623		0.412		0.525
CNT		0.952		0.962		0.903		0.944

toluene conversion on the six different catalysts was bellowed to deep oxidation without CO production, while toluene was oxidized (Fig. 7(b)) after the initial 50 min during which the carbon catalyst was burnt.

3.3.2. NO reduction with toluene

As discussed above, high mesoporous content catalysts show high activity in VOC oxidation at low temperatures. In this section, the activities of the cobalt catalysts in oxidation and reduction reactions were studied simultaneously. The results of previous studies [36,47–49] show that organic compounds, NH_3, and CO can be used in a selective catalyst reactor (SCR) as reductants for NO reduction over noble-metal catalysts. NO reduction on cobalt

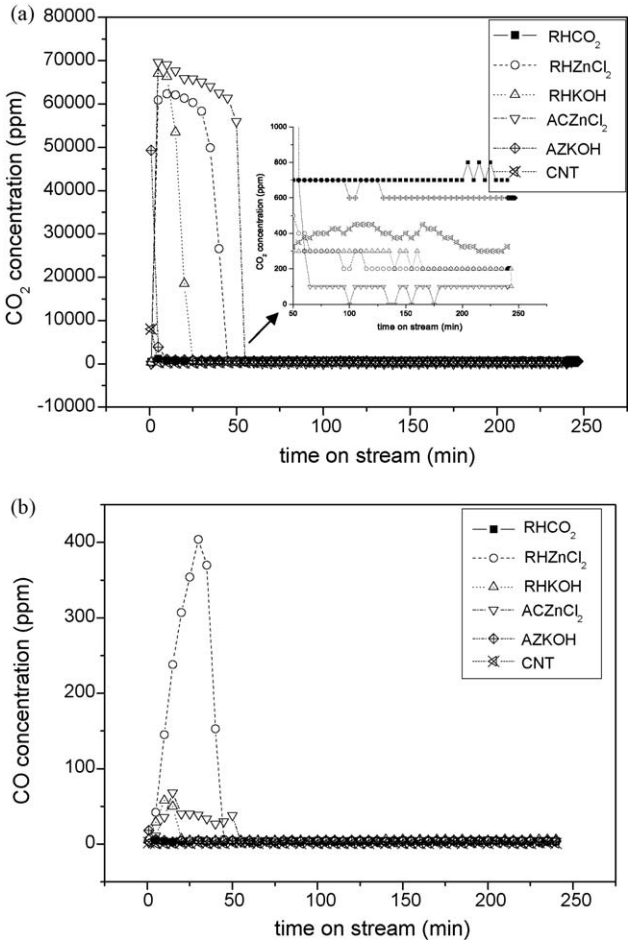

Fig. 7. Variation of gas concentration in the stream with different supports on cobalt catalysts tested at 250 °C: (a) for CO_2, (b) for CO (feed composition: 150 ppm toluene, SV = 40,000 h^{-1}, and 6% O_2 in N_2).

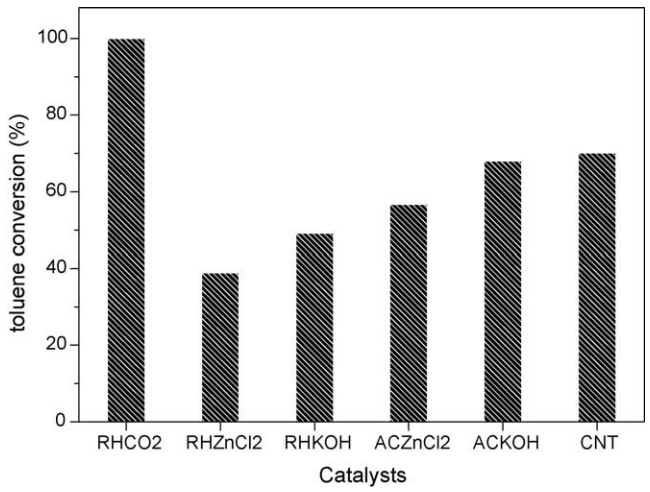

Fig. 8. The toluene conversion with different supports on cobalt catalysts tested at 250 °C (feed composition: 150 ppm toluene, 600 ppm NO, SV = 40,000 h^{-1}, and 6% O_2 in N_2).

catalysts using VOC and CO was investigated and is discussed in this section.

Fig. 8 shows toluene conversion over the six types of cobalt catalysts. From this figure, it is seen that in the presence of NO, the activity of all the catalysts for toluene oxidation decreased; however the $RHCO_2$ catalyst showed the same toluene conversion as before and was recovered 100%. These results were similar to those of previous studies (Fig. 6); in the presence of NO, the activity of cobalt catalysts supported on carbon was observed to be in the following order: $RHCO_2$ > CNT > $ACZnCl_2$ > ACKOH > RHKOH > $RHZnCl_2$.

The NO reduction reaction and the variation of CO_2 concentration during the NO + toluene reaction on cobalt catalysts in a mixture of gases at 250 °C are shown in Fig. 9. The CNT- and $RHCO_2$-cobalt catalysts show better activity for NO reduction than others and were recovered 46% and 10%, respectively, as shown in Fig. 9(a); the conversion efficiencies of these two catalysts were stable during the NO + toluene reaction, whereas those of other catalysts decreased with time. The performance of other catalysts ($RHZnCl_2$, RHKOH, $ACZNCl_2$, and ACKOH) in the NO conversion was reduced with time, and this was due to the low activity caused by the burn-off reaction. A previous study [41] explained that the active phases were combined to form a large size due to the burn-off reaction; this leads to low catalytic activity as the chemical state of cobalt changes. By comparing Fig. 9(b) with Fig. 7(a), it is clear that CO_2 was released for a longer time (100 min) during NO + toluene reaction than during the toluene oxidation in the absence of NO. The longer period of CO_2 release is because of two reasons. One is the burn-off reaction of the support in the presence of oxygen. From the catalyst weight loss shown in Table 4, the weight loss of the different supported catalysts follows the order

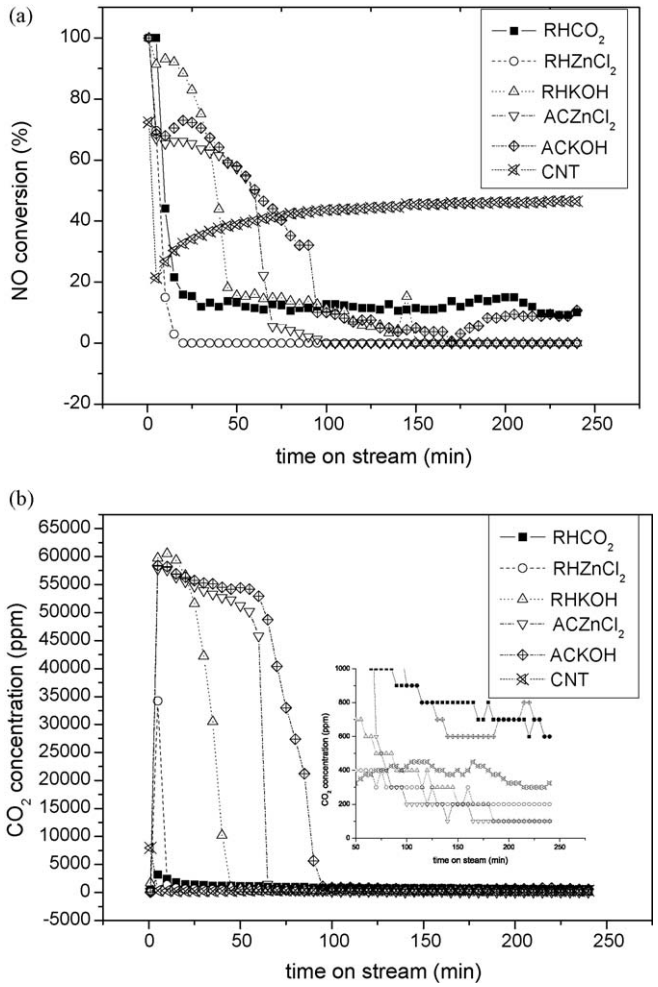

Fig. 9. (a) NO conversion and (b) the variation of CO_2 concentration in the stream with different supports on cobalt catalysts tested at 250 °C (feed composition: 150 ppm toluene, 600 ppm NO, SV = 40,000 h^{-1}, and 6% O_2 in N_2).

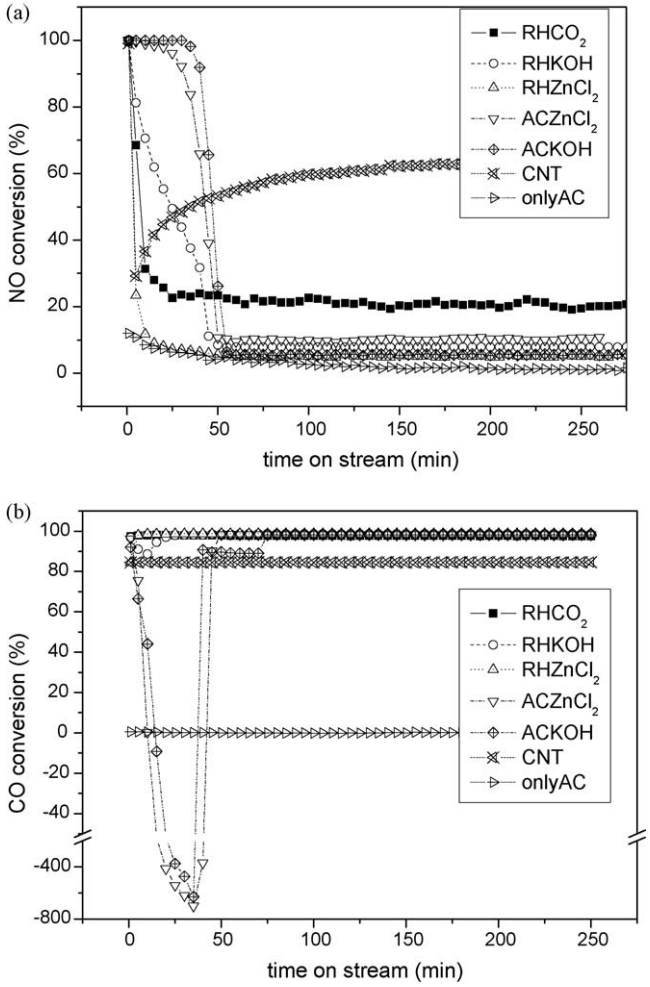

Fig. 10. Variation of pollutant conversion with different supports on cobalt catalysts tested at 250 °C: (a) NO conversion and (b) CO conversion (feed composition: 600 ppm NO, 600 ppm CO, SV = 40,000 h^{-1}, and 6% O_2 in N_2).

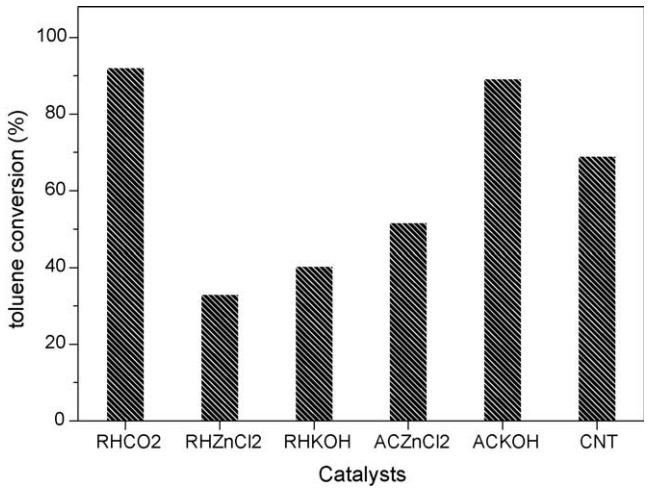

Fig. 11. The toluene conversion with different supports on cobalt catalysts tested at 250 °C (feed composition: 150 ppm toluene, 600 ppm NO, 600 ppm CO, SV = 40,000 h^{-1}, and 6% O_2 in N_2).

of $RHCO_2$ > CNT > RHKOH > ACKOH > $RHZnCl_2$ > $ACZnCl_2$; however, this result does not completely agree with the order observed in the variation of CO_2, as shown in Fig. 9(b). The other reason is the fact that NO reduction is carried out in the presence of toluene. Previous studies [47,48] suggest that NO can be reduced by hydrocarbons; therefore, we speculate that a part of CO_2 is producted from the toluene-NO reaction initially (100 min) on catalysts that decompose easily, such as $ACZnCl_2$ and ACKOH.

3.3.3. NO reduction with CO

It is well known that CO can be a reductant for NO in the absence of oxygen as reported in previous studies [49]; however, in these studies, the oxygen (6%) was always present in flue gas. Therefore, the experiment described below was performed to study the activity of the mesoporous carbon supported cobalt catalysts in gaseous mixtures of CO, NO, and O_2. Fig. 10(a) presents the NO conversion over different supports for the cobalt catalysts in the presence of CO at 250 °C. CNT- and $RHCO_2$-cobalt catalysts show similar efficiencies for NO reduction (Fig. 9(a)). However, in Fig. 11(a), the conversion efficiencies of CNT- and $RHCO_2$-cobalt catalysts were 63% and 22%, respectively, indicating that the catalytic activity was higher with CO as the reductant than that with toluene. In the case of other catalysts, NO reduction was observed to occur with high conversion rate initially (50 min), after which it decreased.

Although all cobalt catalysts showed high catalytic activity for CO conversion from 80% to 100% at 250 °C (Fig. 10(b)), $ACZnCl_2$- and ACKOH-cobalt catalysts initially (50 min) showed a negative CO conversion from −600% to −800%. Negative CO conversions over $ACZnCl_2$- and ACKOH-cobalt catalysts were due to the decomposition of carbon supports during NO + CO reaction. The result showed that CO concentrations increased up to 4500–4800 ppm over $ACZnCl_2$- and ACKOH-cobalt catalysts as compared to other cobalt catalysts during the initial 50 min of the reaction. From this phenomenon, it can be deduced that the carbon supports may be burned off during the NO + CO reaction over $ACZnCl_2$- and ACKOH-cobalt catalysts, as discussed in the Section 3.3.1. The catalyst weights were measured before and after catalytic reaction in different reaction atmospheres and are listed in Table 4. It is also revealed that the weight of the used $ACZnCl_2$- and ACKOH-cobalt catalysts decreased from 0.992 g to 0.361 g and 0.412 g, respectively. Chemical composition of carbon supports and used cobalt catalysts were listed in Table 3. One can see that the element C% was decreased obviously over used $ACZnCl_2$ (91.27% → 60.22%) and ACKOH (91.40% → 64.16%) cobalt catalysts as compared to original carbon supports. This observation revealed that the thermal stability of the commercial AC-based catalysts is lower in NO–CO–O_2 reaction than that in the NO-toluene-O_2 reaction. Therefore, it can be concluded that the burn-off reaction may decrease the catalytic activity during the initial 50 min of the NO reduction, as shown in Figs. 9(a) and 10(a).

3.3.4. Simultaneous removal of NO, CO, and toluene

As discussed above, it was found that the $RHCO_2$- and CNT-cobalt catalysts revealed the highest catalytic activity and stability during NO reduction at 250 °C. On comparing toluene and CO as reductants, although both CO and toluene can effectively serve as reductants in NO reduction at 250 °C, CO showed a better reduction efficiency than toluene for NO conversion. It is known from literature that replacing single compounds with mixtures can lead to considerable changes in the catalytic activity. In order to study

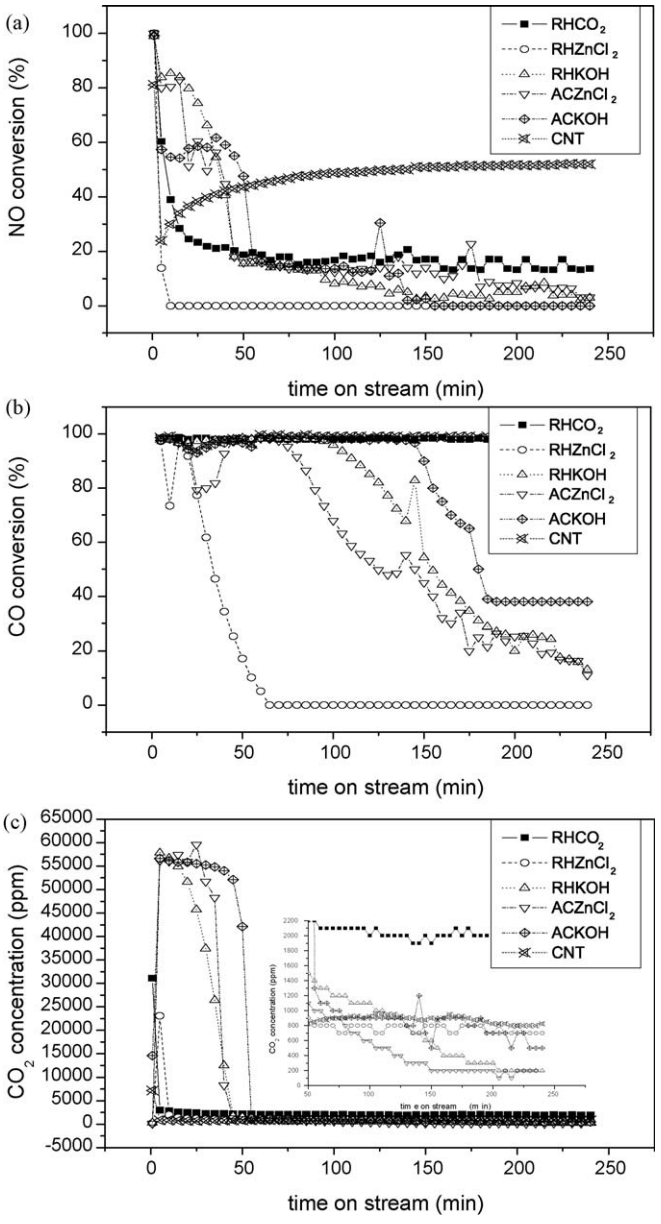

Fig. 12. (a) NO conversion, (b) CO conversion, and (c) the variation of CO_2 concentration in the stream with different supports on cobalt catalysts tested at 250 °C (feed composition: 150 ppm toluene, 600 ppm NO, 600 ppm CO, SV = 40,000 h^{-1}, and 6% O_2 in N_2).

the effect of catalysts on the removal of pollutants from the flue gas, the inlet feed stream selected comprised of 600 ppm of CO, 600 ppm of NO, 150 ppm of toluene, and 6% O_2 in N_2 with a total space velocity of 40,000 h^{-1}. Fig. 11 shows toluene conversion over cobalt catalysts at 250 °C, by comparing Figs. 8 and 11, it is observed that all the cobalt catalysts had the same efficiency for toluene conversion, even after the addition of CO to the reaction atmosphere. The $RHCO_2$-cobalt catalyst exhibited high catalytic activity in VOC oxidation, and it can be concluded that the activity of cobalt catalysts may not be affected by mixture of gases.

Fig. 12 shows NO and CO conversions as functions of time for different cobalt catalysts. The efficiency of the cobalt catalysts in CO oxidation decreases with time, as shown in Fig. 12(b). Except $RHCO_2$- and CNT-cobalt catalysts, all other cobalt catalysts showed a decrease in the rate of CO oxidation with increasing reaction time. $RHCO_2$- and CNT-cobalt catalysts maintained high activity during NO reduction (51% for the CNT-cobalt catalyst) and 100% CO conversion for NO + CO + toluene reaction. By comparing Fig. 12(a) with Fig. 10(a), the NO reduction efficiency of cobalt catalysts ($RHZnCl_2$, RHKOH, $ACZnCl_2$, and ACKOH) is observed to have decreased in the absence of CO oxidation. Fig. 12(c) shows the variation of CO_2 concentration in the stream. In this reaction atmosphere, the CO_2 concentration increased by a factor of two (from 50 min to 250 min) after the catalyst is burnt off, because CO and toluene oxidation occurred at the same time, particularly on $RHCO_2$- and CNT-cobalt catalysts.

4. Conclusions

In this study, porous carbon supports were prepared from rice husks, commercial AC, and CNT via different activation processes. The BET analytical results revealed that mesoporous content of supports was in the order: CNT > $RHCO_2$ > RHKOH > ACKOH > $RHZnCl_2$ > $ACZnCl_2$. More high mesoporous content carbons were advantageous for catalyst preparation by conventional impregnation method; they exhibited good active-site distribution, and the active phases were nanosized (<100 nm).

During toluene oxidation, $RHCO_2$- and ACKOH-cobalt catalysts showed higher conversion efficiency (100%) for deep oxidation at 250 °C than other catalysts. On comparing NO reduction by hydrocarbons with that by CO, CO showed higher conversion efficiency of 63% than toluene (46%) over the CNT catalyst at 250 °C. The toluene and CO conversions in the NO + toluene and NO + CO reactions, respectively, were not significantly different. On studying the simultaneous removal of CO, NO, and toluene, it was observed that the efficiency of NO and toluene removal were not significantly affected by the presence or absence of CO. However, the CO conversion rates decreased with time in the case of catalysts supported on ACKOH, $ACZnCl_2$, RHKOH, and $RHZnCl_2$. The CNT- and $RHCO_2$-cobalt catalysts showed higher catalytic activity and thermal stability at 250 °C than the other catalysts.

References

[1] M.J. Illán-Gómez, A. Linares-Solano, L.R. Radovic, C. Salinas-Martínez de Lecea, Energy Fuels 9 (1995) 97–103.
[2] G. de la Puente, J.A. Menéndez, Solid State Ionics 112 (1998) 103–111.
[3] F. Goncalves, J.L. Figueiredo, Appl. Catal. B 50 (2004) 271–278.
[4] H. Jankowska, A. Swiatkowski, J. Choma, Active Carbon, Ellis Horwood, Chichester, UK, 1991.
[5] H. Tamon, K. Nakagawa, T. Suzuki, S. Nagano, Carbon 37 (1999) 1643–1645.
[6] S. Nagano, H. Tamon, T. Adzumi, K. Nakagawa, T. Suzuki, Carbon 38 (2000) 915–920.
[7] I. Abe, H. Tatsumoto, N. Ikuta, I. Kawafune, Chem. Exp. 5 (1990) 177–180.
[8] Z. Xiongzun, Z. Famnao, L. Lie, L. Qingrong, J. Nanjing Inst. Forest 1 (1986) 19–30.
[9] A. Khan, H. Singh, A.K. Bhatia, Res. Ind. 30 (1985) 13–16.
[10] J. Laine, S. Yunes, Carbon 30 (1992) 601–604.
[11] Z. Hu, M.P. Srinivasan, Y. Ni, Carbon 39 (2001) 877–886.
[12] F. Rodriguez-Reinoso, M. Molina-Sabio, M.T. Gonzalez, Carbon 33 (1995) 15–23.
[13] J.P.L. Walker, Carbon 34 (1996) 1297–1299.
[14] M. Molina-Sabio, M.T. Gonzalez, F. Rodriguez-Reinoso, A. Sepulveda-Escribano, Carbon 34 (1996) 505–509.
[15] E. Arenas, F. Chejne, Carbon 42 (2004) 2451–2455.
[16] H. Benaddi, T.J. Bandosz, J. Jagiello, J.A. Schwarz, J.N. Rouzaud, D. Legras, Carbon 38 (2000) 669–674.
[17] Z. Hu, H. Guo, M.P. Srinivasa, N. Yaming, Sep. Purif. Technol. 31 (2003) 47–52.
[18] M. Molina-Sabio, F. Rodriguez-Reinoso, Colloid Surf. A: Physicochem. Eng. Aspect. 241 (2004) 15–25.
[19] K. Mohanty, D. Das, M.N. Biswas, Chem. Eng. J. 115 (2005) 121–131.
[20] E. Mora, C. Blanco, J.A. Pajares, R. Santamaria, R. Menendez, J. Colloid Interface Sci. 298 (2006) 341–347.
[21] J. Ganan-Gomez, A. Macias-Garcia, M.A. Diaz-Diez, C. Gonzalez-Garcia, E. Sabio-Rey, Appl. Surf. Sci. 252 (2006) 5976–5979.
[22] D. Adinata, W.M.A. Wan Daud, M.K. Aroua, Bioresour. Technol. 98 (2007) 145–149.
[23] T. Kyotani, Carbon 38 (2000) 269–286.
[24] E. Frackowiak, F. Beguin, Carbon 39 (2001) 937–950.
[25] P. Ariyadejwanich, W. Tanthapanichakoon, K. Nakagawa, S.R. Mukai, H. Tamon, Carbon 41 (2003) 157–164.
[26] H. Tamai, T. Kakii, Y. Hirota, T. Kumamoto, H. Yasuda, Chem. Mater. 8 (1996) 454–462.
[27] D. Cazorla-Amoros, D. Ribes-Perez, M.C. Roman-Martinez, A. Linares-Solano, Carbon 34 (1996) 869–878.
[28] J. Yang, Z. Shen, Z. Hao, Carbon 42 (2004) 1872–1875.
[29] J. Hayashi, T. Horikawa, K. Muroyama, V.G. Gomes, Micropor. Mesopor. Mater. 55 (2002) 63–68.
[30] F. Caturla, M. Molina-Sabio, F. Rodríguez-Reinoso, Carbon 29 (1991) 999–1007.
[31] M.Z. Hussein, R.S.H. Tarmizi, Z. Zainal, R. Ibrahim, M. Badri, Carbon 34 (1996) 1447–1449.
[32] N.R. Bishnoi, M. Bajaj, N. Sharma, A. Gupta, Bioresour. Technol. 91 (2004) 305–307.
[33] Y. Guo, J. Qi, S. Yang, K. Yu, Z. Wang, H. Xu, Mater. Chem. Phys. 78 (2003) 132–137.
[34] T.L. Keat, M.M. Atikah, F.Z. Nor, B. Subhash, R.M. Abdul, Fuel 84 (2005) 143–151.
[35] S.J. Wang, W.X. Zhu, D.W. Liao, C.F. Ng, C.T. Au, Catal. Today 93–95 (2004) 714–771.
[36] B. Huang, R. Huang, D. Jin, D. Ye, Catal. Today 126 (2007) 279–283.
[37] T.H. Usmani, T.W. Ahmad, A.H.K. Yousufzai, Bioresour. Technol. 48 (1994) 31–35.
[38] N. Yalcin, V. Sevinc, Carbon 38 (2000) 1943–1945.
[39] J. James, M. Subba Rao, Cem. Concr. Res. 16 (1986) 67–73.
[40] P. Serp, M. Corrias, P. Kalck, Appl. Catal. A 253 (2003) 337–358.
[41] H.H. Tseng, M.Y. Wey, Chemosphere 62 (2006) 756–766.
[42] V. Boonamnuayvitaya, S. Sae-ung, W. Tanthapanichakoon, Sep. Purif. Technol. 42 (2005) 159–168.
[43] J. Zhang, H. Xu, Q. Ge, W. Li, Catal. Commun. 7 (2006) 148–152.
[44] J.C.S. Wu, T.Y. Chang, Catal. Today 44 (1998) 111–118.
[45] C.H. Wang, Chemosphere 55 (2004) 11–17.
[46] E. Gulari, C. Güldür, S. Sompop, O. Somchai, Appl. Catal. A 182 (1999) 147–163.
[47] R. Burch, D. Ottery, Appl. Catal. B 9 (1996) 19–24.
[48] R. Burch, D. Ottery, Appl. Catal. B 13 (1997) 105–111.
[49] D. Mantri, P. Aghalayam, Catal. Today 119 (2007) 88–93.